Teleconnection Linking Asian/Pacific Monsoon Variability and Summertime Droughts and Floods over the United States

K. M. Lau[1] and Hengyi Weng[2]

(March 15, 2000)

To Be Submitted to ***Science***

[1] Climate and Radiation Branch, Laboratory for Atmospheres, Goddard Space Flight Center, NASA, Greenbelt, MD 20771, USA.
[2] General Science Co./SAIC, Beltsville, MD20705, USA.

ABSTRACT

Major droughts and floods over the U.S. continent may be related to a far field energy source in the Asian Pacific. This is illustrated by two climate patterns associated with summertime rainfall over the U.S. and large-scale circulation on interannual timescale. The first shows an opposite variation between the drought/flood over the Midwest and that over eastern and southeastern U.S., coupled to a coherent wave pattern spanning the entire East Asia-North Pacific-North America region related to the East Asian jetstream. The second shows a continental-scale drought/flood in the central U.S., coupled to a wavetrain linking Asian/Pacific monsoon region to North America.

Summertime droughts and floods are among the most costly natural disasters affecting the United States. Yet, compared to wintertime severe weather, the mechanisms of summertime droughts and floods are much less known, and the prospect for long-term prediction is further away. Occurrences of summertime drought/flood over the U. S. continent have been attributed to a large number of factors including the variations of tropical sea surface temperature (SST), extratropical SST, large-scale atmospheric circulation, springtime soil moisture and land-atmosphere hydrology feedback. Some earlier studies (*1, 2*) have suggested the possible influence of El Niño/La Niña. Others have pointed to the larger role played by remote forcings from transient or stationary waves (*3-7*). Up to now, most of the observational or theoretical studies on mechanisms of U.S. droughts and floods have mainly focused on the extreme events of 1998 and 1993 (*6, 8*). However, for unraveling basic mechanisms and exploring predictability, it is important to determine if such events occur episodically, or as manifestations of intrinsic climate modes.

In searching for global climate modes affecting regional droughts and floods processes, the source regions for energy and water have to be considered. During the boreal summer, the Asian monsoon and western Pacific regions constitute the most dominant energy and water sources for the atmospheric general circulation. Previous investigators have noted that a teleconnection pattern, the so-called Pacific-Japan pattern that spans the northern rim of the Pacific Ocean from southern Japan to North America, may be excited by convective heating over the subtropical western Pacific near Philippines during the boreal summer (*9, 10*). Lau and Peng (*3*) and Lau (*11*) showed that a wave train spanning the same regions but with shorter wavelength can be identified as a marginally unstable normal mode of the summertime large-scale monsoon

circulation. They refer to this as the Asian Pacific-North America (APNA) pattern, and suggested that this wavetrain, when forced by tropical heating may contribute to summertime rainfall anomalies over the US continent. A number of authors (*12, 13*), while investigating Asian monsoon, have noted strong trans-Pacific wave signals emanating from the East Asian monsoon regions to North America during periods of severe droughts and floods over East Asia. However, the relationships of these wavetrains to major U.S. droughts and floods have never been firmly established. In this paper, we examine the remote forcing mechanisms for U.S. droughts and floods, with emphases on the teleconnection linking the Asian/Pacific monsoon anomalies and North American climate on interannual timescales.

Observational Data. Our analysis uses monthly rainfall from 102 divisions over the United States (*14*), monthly 500 hPa geopotential height and 850 hPa horizontal wind (*15*), monthly sea surface temperature (SST) (*16*), and monthly global rainfall from CPC (Climate Prediction Center) Merged Analyses of Precipitation (CMAP) (*17*). The seasonal mean for *summertime,* which are used for calculations here, are defined by the average over June-July-August, except for the rainfall that is for the 3-month total. The period for analysis is 1955-98. All the anomalies are calculated as departures from the temporal mean over the 1961-90 base period, except for the CAMP rainfall which base period is 1979-90. To focus on interannual variability, we remove all the variability with timescales longer than 8-years by using a high-pass filter (*18*). The discussion of long term variability (decadal and longer) and its possible modulation of the interannual variability will be presented in a separate paper.

Teleconnection patterns. One-point correlation maps of 500 hPa geopotential height and in SST have been computed for area-averaged summertime rainfall over large number of subregions of the U.S. To various degrees, all subregions show teleconnection signals upstream

in the North Pacific. Here, we only show the results for the central U.S./Midwest region (35°-47°N, 100°-85°W). This region appears to be most susceptible to the ravages of summertime major droughts and floods. It was hardest hit both by the 1988 drought and the 1993 flood, as well as by a recent severe flood in 1998.

Figure 1 shows the one-point correlation maps of 500 hPa geopotential height and SST with respect to the area-averaged rainfall over the aforementioned region (shown by the box in the figure). The following discussion is with respect to flood situation over the central U.S. The sign of the anomalies will be reversed for drought. It is evident from Fig. 1a that rainfall variability in the central U.S. is linked to a distinct wavetrain stretching from East Asia, across the North Pacific to North American. The most pronounced portion of the wavetrain is over the northeastern Pacific and North American sector. A large scale mid-tropospheric low covers much of the central and northern North American continent. This low is sandwiched between two highs, one over southeastern U.S., and one over northwestern Canada. The 500 hPa pattern suggests that excessive rainfall over the central U.S. is associated with strong westerly flow over the area, likely associated with the southward shift of the summertime storm track. Upstream in the central North Pacific, which is connected to the aforementioned continental trough-ridge system, is a wave pattern with a strong low over the Aleutians, a low over the western North Pacific and eastern Asia/Japan area, and a weak high in between. This wavetrain system is similar to the pattern reported by Nitta (*9*) and Lau and Peng (*3*), except the signal here is by design more pronounced over the U.S. where the reference point is chosen.

The sea surface temperature teleconnection (Fig 1b) shows a very pronounced negative SST anomaly located in the central North Pacific, associated with the geopotential low in the 500 hPa wavetrain. A positive SST anomaly area is found over the northeastern Pacific associated with

the geopotential high over northwestern Canada. In the tropical eastern Pacific, there is a broad area of positive SST anomaly, but no apparent El Niño signal. Warmer water is found over the maritime continent/South China Sea region. Both the geopotential height and SST correlation maps suggest a connection of the floods and droughts over the central U. S. to variability in the Asian/Pacific monsoon region (*12*). However, because of the vast span of the wavetrain, it is unlikely that it stems from a single source. Moreover, the one-point correlation maps are unable to separate different mechanisms that may influence the rainfall in this area. As we shall show next, this wavetrain reflects effects from at least two intrinsic climate modes.

Intrinsic climate modes. To examine the relationship of the aforementioned wavetrain to possible recurring summertime rainfall patterns linking the Asian monsoon/North Pacific/North America region, we have carried out Singular Value Decomposition (SVD) analyses (*19*) of the U.S. rainfall and 500 hPa geopotential height.

Figure 2 shows the spatial and temporal structure of rainfall and 500 hPa geopotential height for the most dominant SVD mode (SVD1), which explains 32% of the total squared covariance between the two fields. The spatial rainfall pattern (Fig. 2a) features a dipole linking excessive rainfall over the Midwest region to deficit rainfall over eastern and southeastern U.S., and vice versa. Associated with this flood/drought pattern is a 500 hPa geopotential wavetrain with an approximate regional wavenumber 8 in the East Pacific-North America sector. Over the North American continent, the wavetrain is characterized by a pronounced low over northwestern North America and a high over eastern and southeastern U.S. This wave pattern is linked upstream to a gigantic elongated extratropical trough-ridge system stretching from East Asia across the entire north Pacific. This pattern is similar to the teleconnection pattern associated with the north-south shift of the East Asian subtropical jetstream, induced by heating over

Southeast Asia (*12*). The principal components (PC, Fig. 2c), which describe the temporal variation of the spatial patterns, indicate that this mode accounts a large fraction of the U.S. rainfall variation during the summer of 1993 when the Midwest experienced a severe flood while the eastern and southeastern U.S. suffered a drought. However, this mode has negligible role in the 1988 drought.

The spatial rainfall pattern of the second mode (SVD2) (Fig. 3a) shows widespread, continental-scale rainfall anomalies of the same sign centered over the central U.S., with anomalies of the opposite sign over the northwestern and the southwestern U. S. The associated 500 hPa geopotential height pattern (Fig. 3b) features a pronounced wavetrain spanning the entire Pacific with an "apparent" source over East Asia/Japan region. Much of the continental North America is under the influence of a pronounced high centered just to the northwest of the Great Lakes. An equally prominent low sits over the northwestern North America and Alaska. The PCs (Fig. 3c) show that this mode reflects drought conditions over the central U.S. (large positive PC) during 1983 and 1988. This mode also contributes to the flood over the Midwest (negative PC) during 1993, while partially cancels the degree of the drought in eastern and southeastern U. S., where the drought would be much more severe if it were due to the influence of SVD1 alone. During the recent 1998 summertime flood in the central U.S. and drought in eastern and southern U.S., both SVD1 and SVD2 appear to play important roles.

Physical interpretations. The above results show that the one-point teleconnection signal associated with the central U.S. droughts and floods may stem from the interplay of two distinct summertime climate modes, both of which may have sources in the Asian monsoon region. To further explore these connections, regressions of the rainfall PCs for SVD1 and SVD2 against

the 850 hPa wind and SST and the correlation between the PCs and CMAP global rainfall are computed and shown in Fig. 4.

Figures 4a and 4b show the 850 hPa wind and *global* rainfall patterns associated with SVD1 mode, respectively. Clearly, SVD1 depicts a global, or more strictly a *Pan-Pacific,* drought/flood pattern. Over North America, the pattern covers not only the U. S., but also much of northern and northwestern Canada. Excessive rainfall over the central U.S./Midwest and the simultaneous occurrence of deficient rainfall over eastern and southeastern U. S. is affected by increased southerly low-level flow, bringing moisture from the Gulf of Mexico to the Midwest. This is facilitated by the formation of an anomalous low-level anticyclone over the east coast. Remarkably, this North America rainfall anomaly dipole is linked to zonally banded rainfall anomalies that stretched across the entire North Pacific from East Asia, with enhanced (reduced) rainfall generally coinciding with regions of low-level cyclonic (anticyclonic) flow. In the tropics, there is a weaker signal indicating generally enhanced rainfall in a large fetch of enhanced westerlies in the central and eastern equatorial Pacific. Between these two rainbands is an elongated dry zone between 10°-30°N strentching eastward and slightly poleward, from South Asia across the subtropical Pacific to southeastern U. S. The regressed SST anomaly pattern for SVD1 (Fig 4c) suggests some degree of El Niño influence, as evidence in the positive SST over the equatorial eastern and central Pacific, underlying anomalous westerlies and increased precipitation. Another prominent feature in the Fig. 4c is the presence of an extensive cold region in the extratropical Pacific (near 40°N), coinciding with anomalous low-level westerlies and reduced rainfall. These features are dynamically consistent with forcing of the extratropical ocean by enhanced evaporation and upper-ocean mixing, through increased surface wind and

reduced shortwave radiation through increased cloudiness associated with excessive precipitation (*20*).

For SVD2, the associated 850 hPa wind and rainfall patterns also suggest a global underpinning (Figs. 5a and 5b). In the U.S. continent, there is a widespread drought area centered over the middle of the Great Plains. The associated low-level flow indicates the establishment of a large anticyclone over northeastern North America coupled to an equally extensive cyclone over the Gulf region. This anticyclone/cyclone couplet induces anomalous low-level easterlies in southern U.S., effectively cutting off moisture supply from the Gulf of Mexico. As part of the continental-scale system, a well-developed cyclonic circulation is found over northwestern North America, featuring southerly flow that feeds moist oceanic air into the region, resulting in excessive rainfall. This continental wave pattern is a part of a much larger and well-organized wavetrain emanating from the subtropical western Pacific, in an arc path across the north Pacific to North America. Regions of enhanced (reduced) rainfall appear to align along the direction of the wavetrain, coinciding with low level cyclonic (anticyclonic) circulation, that can be traced back to enhanced convection over Indo-China. In particular, the anticyclonic flow over the subtropical western Pacific near the Philippine, which is associated with prevailing easterly flow in the equatorial western and central Pacific, has been identified as one of the key features of the Asian summer monsoon variability affecting droughts and floods in China, Japan and Korea (*12*). This wavetrain pattern is associated with substantial changes in extratropical SST, with positive (negative) SST anomalies underlying the anticyclones (cyclones) (Fig. 5c). This suggests that SST anomalies there be forced by atmospheric circulation. There is only a weak SST signal in the tropical eastern Pacific. Hence, this mode is

unlikely dependent, at least not directly, on El Niño/La Niña, but rather arises from interannual variability of the Asian monsoon.

Conclusion. The results presented in this paper suggest that major summertime droughts and floods over the U.S. are parts of Pan-Pacific rainfall anomaly patterns. In order to better understand the mechanisms of floods and droughts over the U. S., a global view has to be considered. Here, we have only begun to explore such a view focusing on the possible interannual teleconnections and impacts by the Asian monsoon variability during the summertime. It is likely that such teleconnections may have evolved from preceding spring or winter seasons, as well as occurring on subseasonal timescales. Identifying these early season teleconnection signals will be the key to improve summertime drought and flood forecasts over the U.S. The impact on the interannual teleconnection by decadal variations in the Pacific is another critical area that deserves more research in order to better determine the predictability of the U.S. summertime droughts and floods.

References and Notes

1. K. E. Trenberth, G. W. Branstator, P. A. Arkin, *Science*, **242**, 1640 (1988); K. E. Trenberth, G. W. Branstator, *J. Climate*, **5**, 159 (1992); K. E. Trenberth, C. J. Guillemot, *J. Climate*, **9**, 1288 (1996).
2. T. N. Palmer, Č. Braković, *Nature*, **338**, 54 (1989).
3. K.-M. Lau, L. Peng, *J. Climate.*, **5**, 140 (1992).
4. M. Ting, H. Wang, *J. Climate*, **10,** 1853 (1997).
5. K.-C. Mo, J. N. Paegle, R. W. Higgins, *J. Climate*, **10**, 3028 (1997).
6. A. Z. Liu, M. Ting, H. Wang, *J. Atmos. Sci.*, **55**, 2810 (1998).
7. R. W. Higgins, Y. Chen, A.V. Douglas, *J. Climate*, **12**, 653 (1999).

8. P. Chen, M. Newman, *J. Climate*, **11**, 2491 (1998).

9. T. Nitta, *J. Met. Soc. Japan*, **65**, 373 (1987).

10. R. Huang, *Adv. Atmos. Sci.*, **2**, 81-92 (1985).

11. K.-M. Lau, *J. Meteor. Soc. Japan*, **81**, 211 (1992).

12. K.-M. Lau, K. M. Kim, S. Yang, *J. Climate* (in press) (2000).

13. C. Li, L. Zhang, *Chinese J. Atmos. Sci.*, **23,** 111 (1999).

14. The 102-division precipitation data were from the National Climate Data Center through CPC. We are thankful to Y. He for many helps.

15. The NCEP/NCAR reanalysis data. Kalnay, et al., *Bull. Amer. Meteor. Soc.*, **77**, 437 (1996).

16. The GISST2.3b data set was provided by Dr. D. E. Parker and J. Arnott at the Hadley Centre for Climate Prediction Research, United Kingdom.

17. P. Xie, P. A. Arkin, *Bull. Amer. Meteor. Soc.*, **78**, 2539 (1997).

18. The bandpass routine was from Dr. J. Ahlquist at the Meteorology Department of the Florida State University.

19. C. S. Bretherton, C. Smith, *J. M. Wallace, J. Climate*, **5**, 541 (1992).

20. N. C. Lau, M. J. Nath, *J. Climate*, **9**, 2036 (19976)

21. The authors are thankful to Drs. K.-M. Kim and J. Zhou for providing help in certain data processing. This work was supported by the Global Modeling and Analysis Program and the Earth Observing System Interdisciplinary Investigation Program of the NASA/Office Mission to Planet Earth.

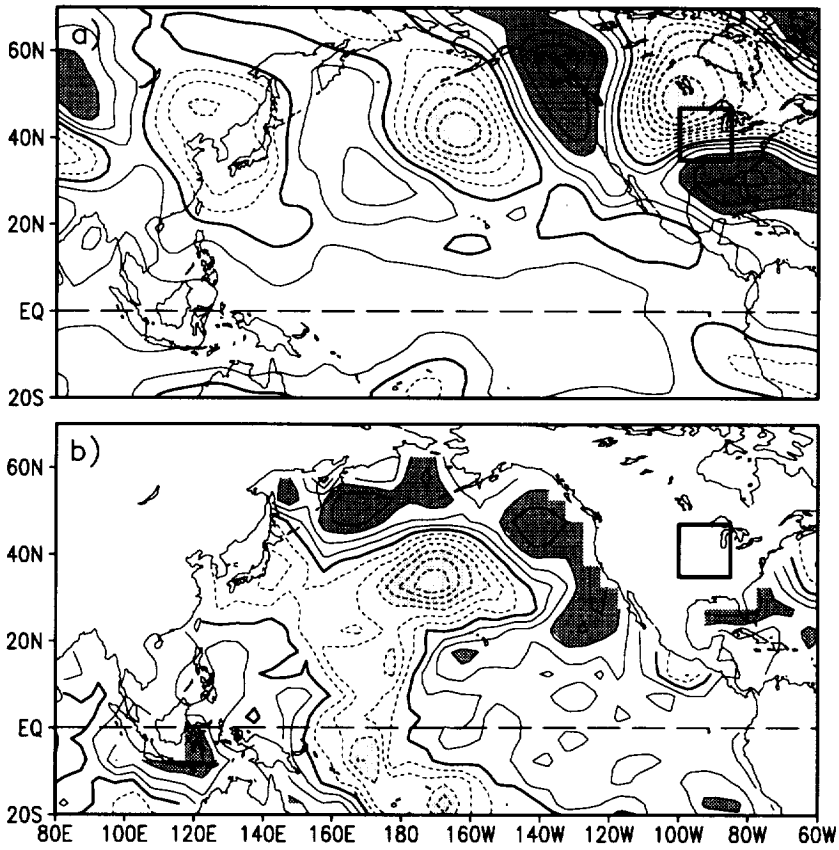

Figure 1. (a) Correlation between area averaged rainfall in the box (100°-75°W, 35°-47°N) and 500 hPa geopotential height anomalies, and (b) correlation between the same rainfall and SST anomalies, for the period of 1955-98 summertime. Contour interval is 0.1. Positive (negative) correlation coefficients with magnitude larger than 0.3 are dark (light) shaded.

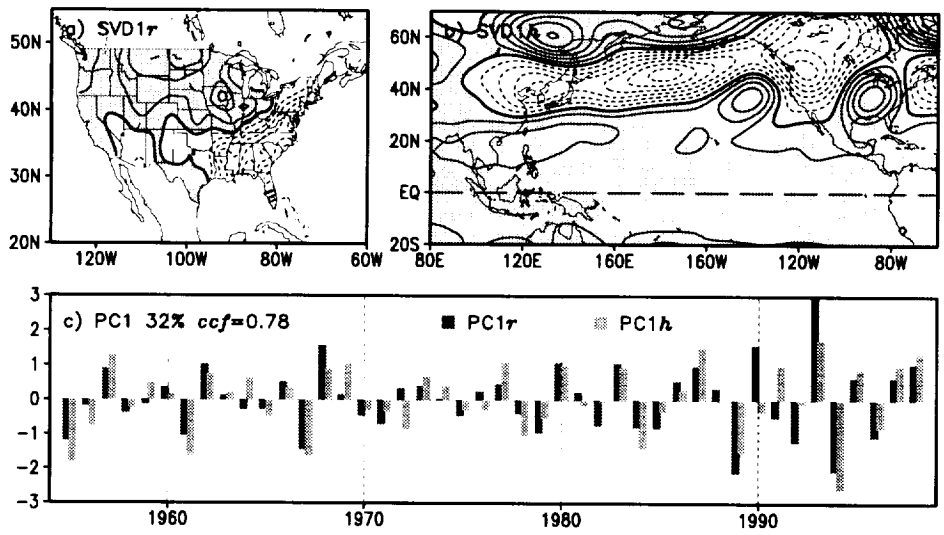

Figure 2. SVD1 between 500 hPa geopotential height and U.S. rainfall anomalies for 1955-98 summertime. (a) rainfaill spatial pattern (SVD1*r*), (b) geopotential height spatial pattern (SVD1*h*), (c) principal components of rainfall (PC1*r*) and geopotential height (PC1*h*). Both PC1 have been normalized by their standard deviations (σ), so that each correspoinding spatial pattern in (a) and (b) represents 1-σ loading of that variable.

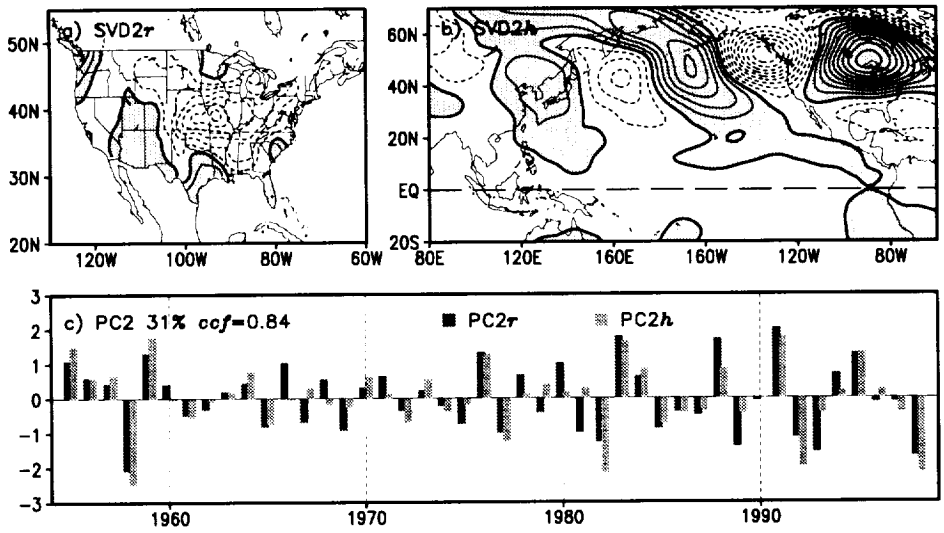

Figure 3. Same as Fig. 2, except for SVD2.

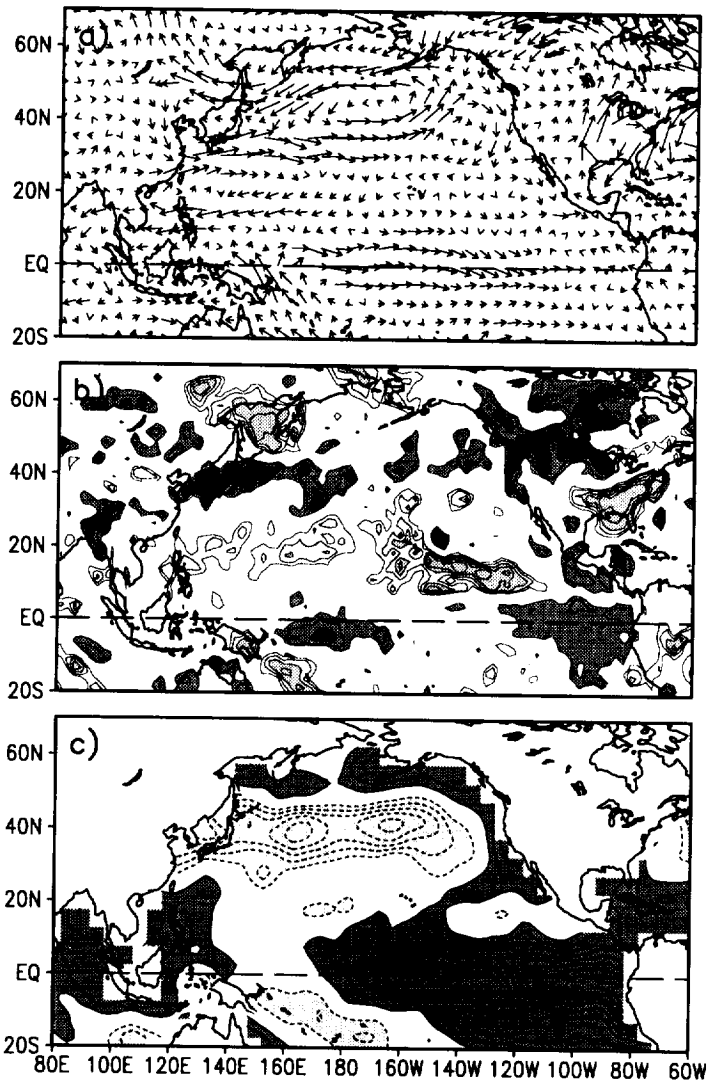

Figure 4. Spatial patterns of 850 hPa horizontal wind, CMAP rainfall, and SST related to SVD1 mode. (a) Regression of PC1*r* against the wind anomaly for the period of 1955-98 (unit: ms^{-1}/σ). (b) correlation between PC1r and CMAP rainfall anomaly for the period of 1979-98. Wetter (drier) than normal are dark (light) shaded, i.e., correlation values larger than 0.3 are shaded. (c) regression of PC1r against SST anomaly for the period of 1955-98 (interval: $0.5°C/\sigma$). Positive (negative) values greater than 0.5 are darker (light) shaded.

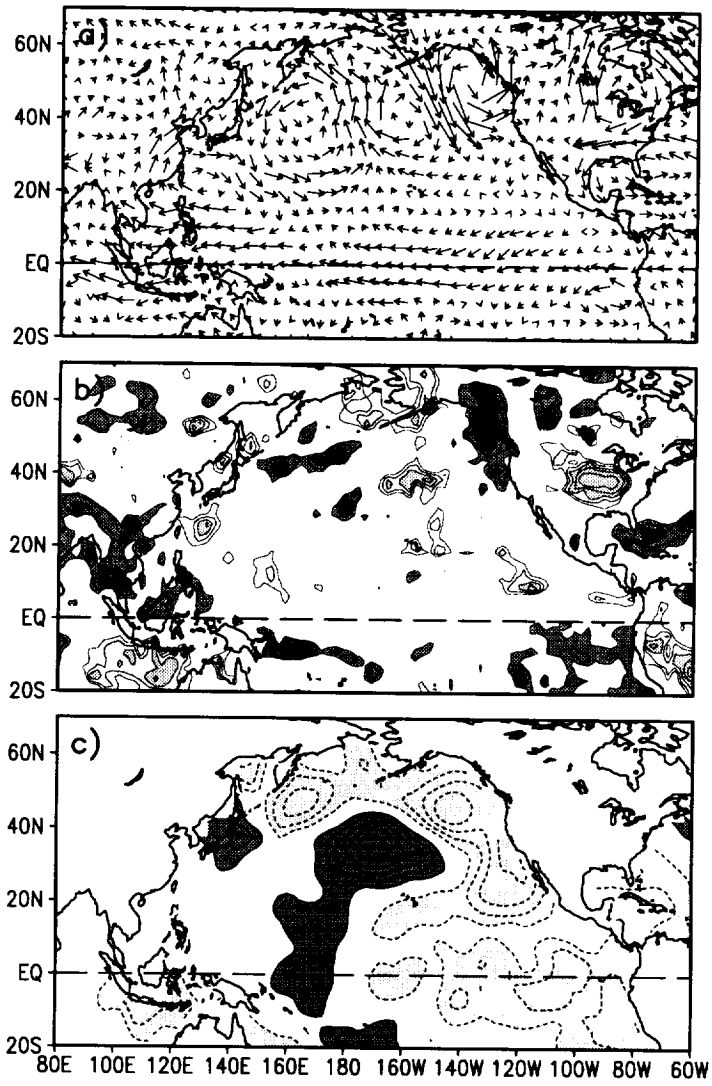

Figure 5. Same as Fig. 4, except for SVD2.